Reaction-Diffusion Dissipative Systems – Detailed Stability Analysis – Pattern of Growth and Effect of Inhomogenity

P. J. Nandapurkar and V. Hlavacek
Chemical Engineering Department, State University of New York at Buffalo, Buffalo, New York 14260, USA

J. Degreve, R. Janssen, and P. Van Rompay
Katholieke Universiteit Leuven, Belgium

Z. Naturforsch. **39 a**, 899–916 (1984); received May 4, 1984

A detailed stability analysis of the one dimensional steady state solutions for the Brusselator model under the conditions of diffusion of initial (non-autocatalytic) components has been performed both for zero flux as well as fixed boundary conditions. In addition to subcritical as well as supercritical bifurcations, situations have been observed where all solution branches at a bifurcation point are unstable. A case of degenerate steady state bifurcation (2 solutions emanating from the same bifurcation point) has also been noticed. A transient simulation of the system in growth reveals the importance of growth rate on the pattern selection process and suggests that the selection of branches at a bifurcation point may be influenced by perturbations/fluctuations. It also indicates that a stability analysis of the bifurcation diagram alone cannot decide the state of the system in a transient process, and under certain situations complex behavior may be observed at limit points.

Numerical calculations on coupled cells indicate that a heterogenity in the system can introduce multiple (two) time scales in the system. As the ratio of time scales increases, aperiodic or irregular oscillations are observed for the 'fast' variable. A combination of cells with one cell in a steady-state mode and the other in a periodic motion results in a combined motion of the entire system. For a distributed parameter system, a heterogenity can cause development of sharp local concentration gradients, alter the stability properties of steady state as well as periodic solutions and can cause partitioning of the system.

1. Introduction

The phenomenon of self-organization, i.e. the formation of new structures from an initially homogeneous medium are of great importance in various fields such as fluid mechanics, biology, chemistry, applied mathematics, chemical engineering, etc. Turing [1] was probably the first one to offer a possible explanation as to how structures may arise in living beings through the mechanism of morphogenesis. He developed a mathematical model for morphogenesis which consisted of an autocatalytic chemical network coupled to diffusion. Several models have been proposed afterwards on this basic idea of coupling between nonlinear kinetics and diffusion to explain the formation of patterns [2–5]. The trimolecular autocatalytic reaction mechanism due to Prigogine and Lefever [2], also referred to in the literature as the "Brusselator", has been subjected to many theoretical investigations to understand the breaking of symmetry which leads to the formation of spatial or spatiotemporal patterns. By making use of the bifurcation theory, Auchmuty and Nicolis [6] and Herschkowitz-Kaufman [7] have constructed the steady state (s. s.) solutions for this model for the case of zero flux and fixed boundary conditions, respectively. These authors have also studied the stability of the primary bifurcating solutions analytically. Boa and Cohen [8] have analyzed the asymptotic behavior of small amplitude solutions near the primary bifurcation point. Kubicek et al. [9] have numerically constructed the bifurcation diagram for this model through the technique of continuation and studied the stability of s. s. solutions. Hlavacek et al. [10] and Janssen et al. [11] have systematically constructed the bifurcation diagram for this model under the conditions of diffusion of the initial (non-autocatalytic) components. The bifurcation diagrams, usually constructed through

Reprint requests to Prof. V. Hlavacek, Chemical Engineering Department, State University of New York at Buffalo, Buffalo, New York 14260, USA.

0340-4811 / 84 / 0900-0899 $ 01.30/0. – Please order a reprint rather than making your own copy.

the s. s. analysis of the governing equations, indicate the number of the s. s. solutions at a particular value of the bifurcation parameter. However, not all the solutions existing simultaneously are stable and since one is normally interested in the asymptotic or the long term behavior, the stability analysis of the s. s. solutions assumes importance. It has been shown by Sattinger [12], for the case of uniform thermodynamic solutions, that supercritically bifurcating solutions are stable while subcritical bifurcations are unstable. Kubicek et al. [13] have verified these conclusions for the case of bifurcating solutions for the Brusselator model under the conditions of infinite diffusion coefficients for the initial components. Nandapurkar and Hlavacek [14], while numerically studying the stability of the s. s. solutions for this model (under the conditions of finite diffusion coefficient of the initial components) observed that low amplitude as well as high wave number solutions at low system size are unstable. However, they have investigated the stability of a few bifurcating branches only. In general, it is observed that no guidelines exist for predicting the stability of the branches bifurcating from nonhomogeneous basic solutions and branches bifurcating from secondary solutions (tertiary bifurcations), and that the mechanism of stability exchange at high order singularities is not properly understood.

It is known that the patterns generated by the nonlinear reaction-diffusion equations display a marked dependence on the size of the domain and are of importance in the development of biological systems. Typically, as the system evolves, the character of the structure (solution) changes along the bifurcation diagram and the patterns are selected as per their stability characteristics. However, it is of importance to know which of the patterns are selected from the existing patterns as the system grows at a finite rate. It is, therefore, required to carry out the transient simulation of the system in growth in collaboration with the stability analysis of the bifurcation diagram. This will help to (i) form certain guidelines for the selection of favored branches (ii) understand the behavior of the system in growth and (iii) analyze the effect of growth rate on the evolution process.

In the majority of the works reported above, the system has been considered to be ideal (isotropic). However, in real situations, heterogenities often exist which can affect the properties of the system locally or globally. For example, in the chemical engineering context, a catalyst can have sites of variable activity. Such heterogenities can often modify the behavior of the system as a whole. This has been observed in experiments with the Belousov-Zhabotinsky reaction where Winfree [15] noted that the spatial patterns, which consisted of spiral rotating waves could be initiated by heterogenities in the form of a catalytic particle (dust) in the system or by localized heating (thermal heterogenity). Tyson and Fife [16] have tried to explain the formation of these spatial patterns on the basis of a rate constant, which is dependent on space (a case of kinetic heterogenity). Jensen and Ray [17] have investigated the effect of a 'physical' heterogenity (nonuniform diameter of a catalytic wire) to show that temperature waves could be initiated and propagated by this configuration. A similar heterogeneous situation is also possible for an autocatalytic reaction, wherein, due to poisoning, the rate constant may vary spatially or temporally. The Brusselator model, which represents an autocatalytic reaction can, therefore, be analyzed from this point of view. To our knowledge, no such work has been reported on this aspect.

Therefore, in this paper, we are going to investigate in detail the stability of the s. s. solutions for the Brusselator model, report on the transient simulation studies for continuously varying length (the bifurcation parameter in the model) and also study the effect of localized heterogenities in the system on the structure of solutions for this model. Since a lumped parameter system is a first approximation to the distributed parameter system, we initially study the effect of heterogenity for the case of two coupled cells, in each of which a Brusselator mechanism prevails and then try to extend the analysis for a distributed parameter case.

2. Governing Equations and the Boundary Conditions

The following reaction-diffusion equations are obtained for the Brusselator model after setting all forward rate constants to unity and neglecting the reverse reactions.

$$\partial A/\partial t = -A + D_A \nabla^2 A\,, \tag{1}$$

$$\partial X/\partial t = A + X^2 Y - (B+1)\,X + D_x \nabla^2 X\,, \tag{2}$$

$$\partial Y/\partial t = B X - X^2 Y + D_y \nabla^2 Y\,. \tag{3}$$

In these equations the components X and Y denote the intermediate species while A and B represent the initial non-autocatalytic components. We consider B to be maintained uniform in space by some external means or through $D_B \to \infty$. For the component A, Dirichlet boundary conditions are considered with A at the boundary being 2.0. In the case of components X and Y, both Dirichlet as well as Neumann boundary conditions are considered with $X = A$ and $Y = B/A$ and zero flux at the boundaries respectively. One can easily observe that (1) is linear and has an analytical solution which has been used in the subsequent calculations.

3. Results

3.1. Stability Analysis of the Steady States

The linear stability of the s. s. solutions to Eqs. (1) to (3) can be determined by linearizing around the nonuniform steady states and calculating the eigenvalues of the resulting matrix. For this purpose the system of the partial differential equations (1) to (3) can be converted to a large system of ordinary differential equations (in general 3Xn) by a high order discretization or orthogonal collocation technique can also be used. The eigenvalues of the resulting matrix can be evaluated via a suitable Q−R decomposition routine. Instability is indicated whenever at least one eigenvalue has a positive real part. Another technique to study the stability behavior is the numerical simulation of the full partial differential equations represented by (1) to (3). In this case, the transient solution obtained at $t \to \infty$ is considered as the stable steady state solution (unless the system shows periodicity). We have used this technique in our analysis. Equations (2) and (3) represent a set of coupled, nonlinear, parabolic type of partial differential equations and we have solved them by a high order finite difference technique. For this purpose, the spatial derivative has been approximated by a high order formula which results in an accuracy $O(h^4, k^2)$ with only 3 mesh points in space. The numerical s. s. solutions calculated earlier in [10] and [11] were perturbed by about 0.1% and this perturbed solution was then used as the initial profile for the purpose of transient simulation. The transient solution, obtained at $t \to \infty$, has been subjected to an additional criterion for ensuring the stability of the resulting steady state. This criterion is a numerical version of the general macroscopic evolution criterion as mentioned in [7]. According to it, the following inequality should be statisfied at the s. s.

$$T = \frac{\mathrm{d}_x P}{\mathrm{d}t} = -R \int \sum (\dot{C}_i)^2 c_i^{-1} \, \mathrm{d}r \leqq 0 \, .$$

In our numerical simulations, the value of T for the solution at $t \to \infty$ has been found to be about 10^{-12}.

The results of the stability analysis, for the case of fixed boundary conditions, have been displayed on bifurcation diagrams (1) to (10) taken from [11]. The solid lines in these figures denote asymmetric profiles while the dotted lines indicate symmetric solutions. The portion of a bifurcating branch which has been drawn thin indicates the stable region. These figures reveal the importance of limit and bifuration points in the stability behavior of distinct solution branches. The conclusions, based on these figures, can be formulated in the following way:

(i) At a bifurcation point (which is a junction of 4 or more half rays of solutions), the half rays corresponding to the symmetric solution branches are unstable. In other words, the symmetric solution branches are not stable before and beyond a bifurcation point. For example see the bifurcation points E_1, F_1, J_1 and J_2 in Fig. 1, C_2 and F_2 in Fig. 4 and C_1 in Figure 6.

(ii) It can be gathered from bifurcation points E_2 in Fig. 7 and D_1 and D_2 in Fig. 4 that at a bifurcation point, the symmetric solution branches can be unstable both before and beyond the point of bifurcation.

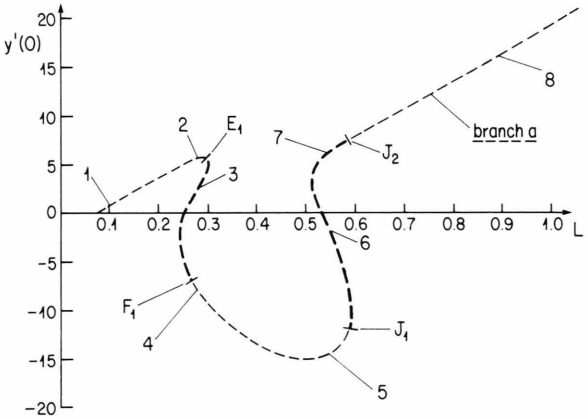

Fig. 1. Bifurcation diagram, branch a (symmetric solutions).

(iii) The asymmetric solution branches cannot change their stability behavior at bifurcation points. This is a consequence of the nature of bifurcations symmetric-asymmetric (two mirror symmetric solutions collapsing into symmetry). In our particular bifurcation diagram, we have observed but one branch of asymmetric solutions which is stable both before and beyond a bifurcation point (bifurcation point C_1 in Figure 6)). More specifically, at the bifurcation points, we have observed the following configuration of half rays as shown in Figure 11. In this figure sketches (a), (c), (g), and (h) show subcritical bifurcations while sketch (d) shows a supercritical bifurcation to the right. Situations (e), (i) and (j) show interesting behavior in the sense that all bifurcating branches at these bifurcation points are unstable. The same behavior is also noticed for the bifurcation points, SB1, TB1 and TB2 in Figure 13. It is apparent that such a situation takes place when two s. s. bifurcation points collapse into one. By this argument it can be easily seen that by a suitable change of parametes, the unstable closed curve portion of the sketch (i) can yield an isolated branch of solutions.

We have also tried to verify stability criterion of Sattinger [12] for the case of non-uniform basic solution. For this purpose, we call the primary branch a (Fig. 1) as the basic branch of solutions. At the bifurcation point E_1 on this branch (Fig. 7), a subcritical bifurcation leads to an unstable closed curve solution. The same also applies for the bifurcation point J_1. The bifurcation points F_1 in Fig. 2 and J_2 in Fig. 8 also agree with the analytical predictions that bifurcations to the left are unstable while the solutions evolving to the right are stable. The stability of solutions emanating from the points of secondary and tertiary bifurcations has also been considered from this point of view. At the bifurcation point C_2 on branch g (Fig. 5), a subcritical bifurcation leads to the evolution of the unstable branch c while, from the Fig. 6, it can be inferred that a supercritical bifurcation (to the right) on branch b leads to the stable branch c. From these general observations, it can be concluded that the guidelines predicted by the analytical methods for the stability of primary bifurcating solutions also seem to hold for the case of higher bifurcations. A global view of the stability (superposition of Figs. 1 to 10) indicates that most of the calculated s. s. solutions are unstable. For example, of the 13 reported

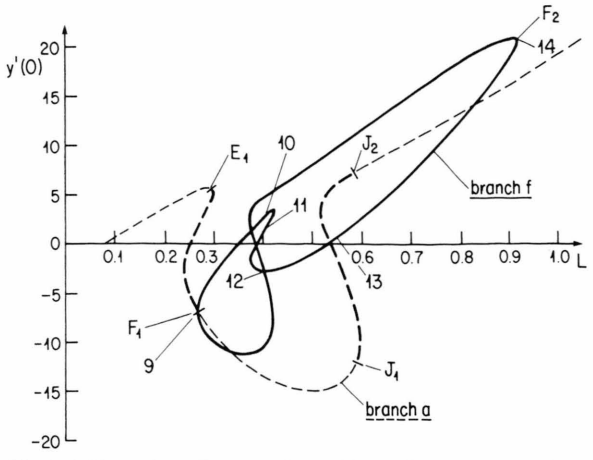

Fig. 2. Bifurcation diagram, branching of symmetric solutions (branch f).

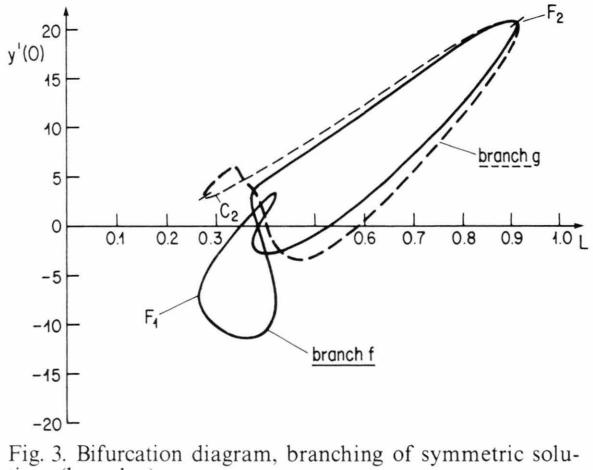

Fig. 3. Bifurcation diagram, branching of symmetric solutions (branch g).

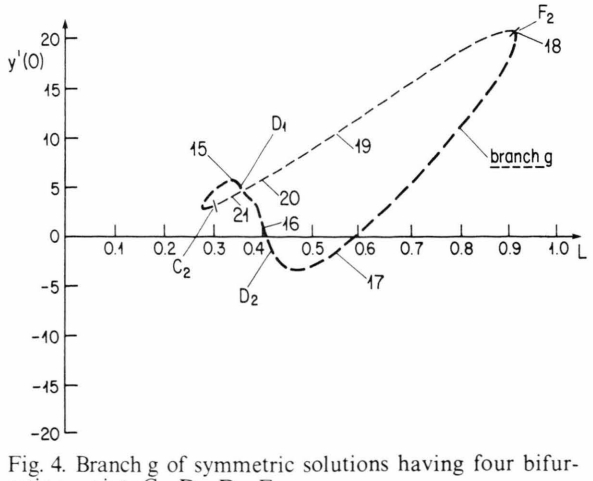

Fig. 4. Branch g of symmetric solutions having four bifurcation points C_2, D_1, D_2, F_2.

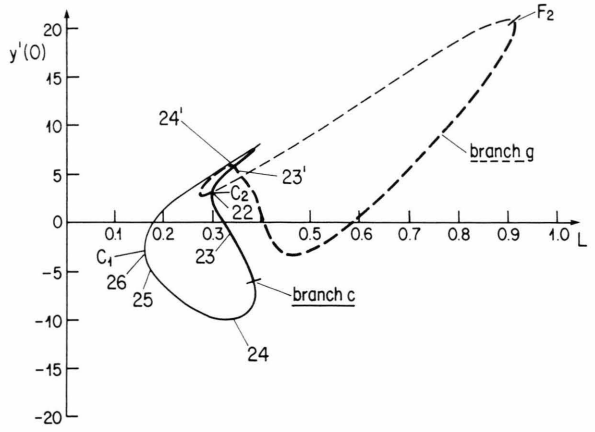

Fig. 5. Bifurcation diagram, branching of asymmetric solutions (branch c).

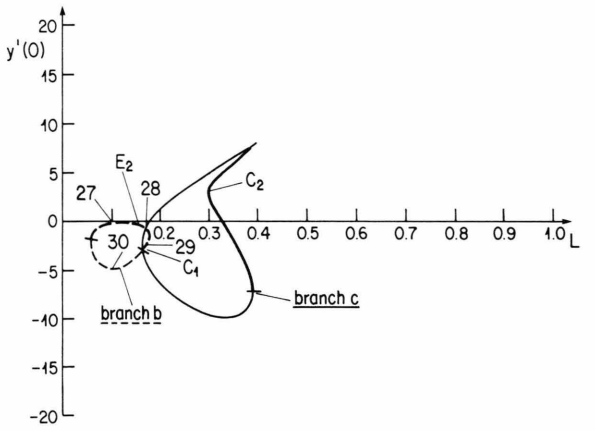

Fig. 6. Bifurcation diagram, branching of asymmetric solutions (branch b).

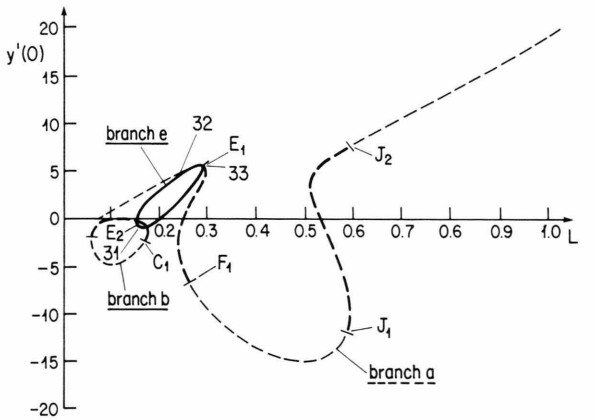

Fig. 7. Bifurcation diagram, branching of asymmetric solutions (branch e).

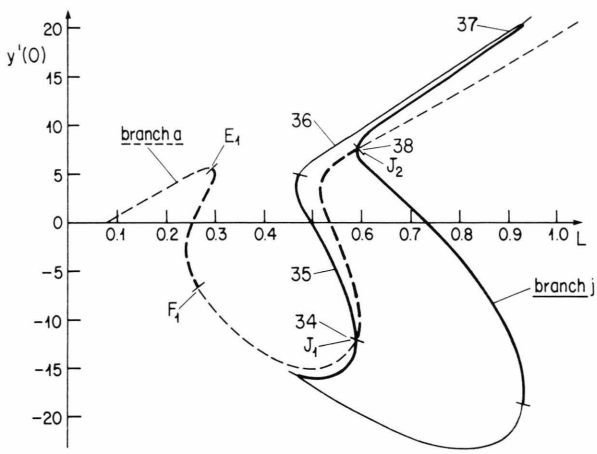

Fig. 8. Bifurcation diagram, branching of asymmetric solutions (branch j).

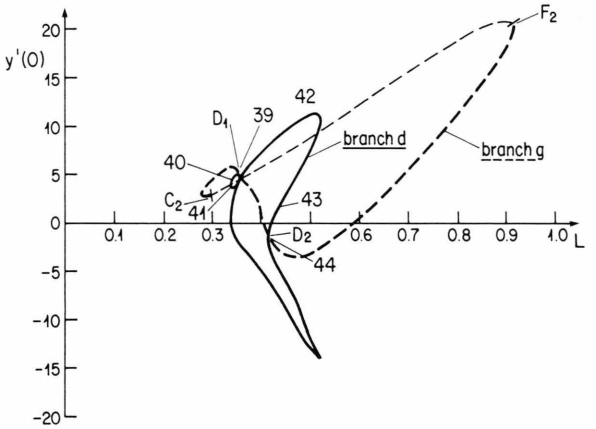

Fig. 9. Bifurcation diagram, branching of asymmetric solutions (branch d).

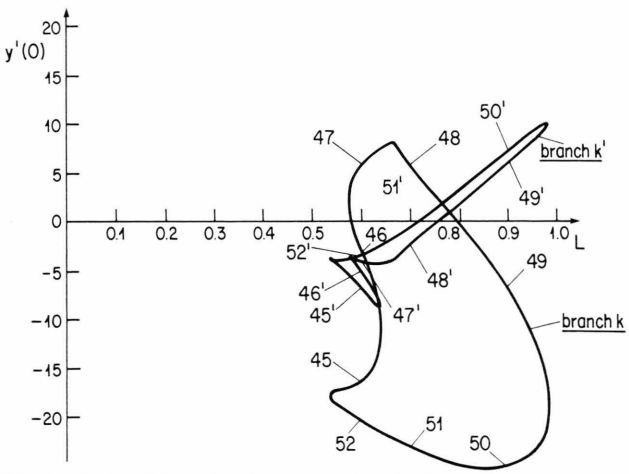

Fig. 10. Isolated branch of asymmetric solutions (branch k, k').

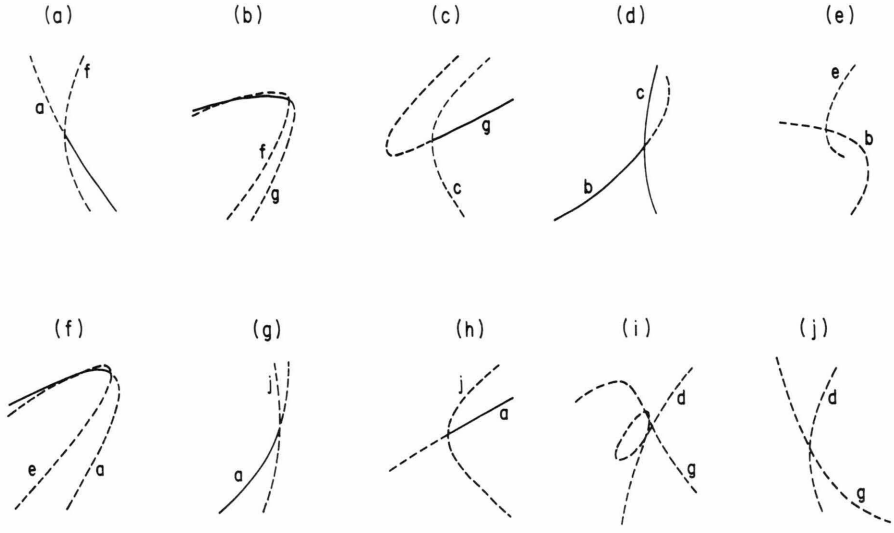

Fig. 11. Stability behavior near bifurcation points. ··· uncertain behavior; --- unstable solutions; —— stable solutions.

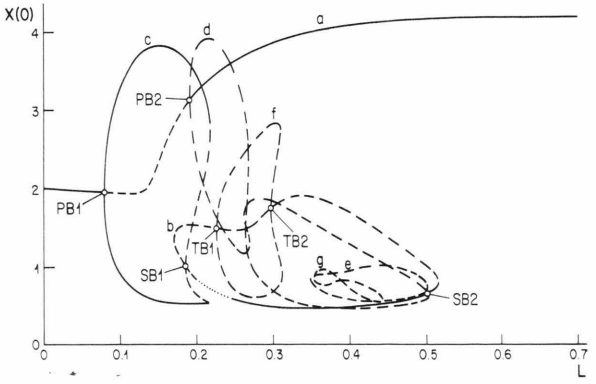

Fig. 12. Bifurcation diagram, zero flux boundary conditions. —— stable solutions, --- unstable profiles.

s. s. solutions, only 4 are stable at $L \cong 0.7$. Another point of interest here is the observation that the solutions which have high derivatives at the boundary have a higher chance of asymptotic stability as compared to the others and the isolated solution branch K (Fig. 10), as calculated earlier in [11], is completely unstable inspite of a number of limit points. One can also notice the stabilization of primary unstable branches through the mechanism of secondary bifurcations from these figures.

The results of stability analysis for the case of Neuman boundary conditions are shown in Figure 12. One can again note here that most of the calculated s. s. solutions are unstable, stable solutions either have a very high or low amplitude and the stability exchange either takes place at limit or bifurcation points. A supercritical bifurcation on the primary branch a leads to stable solutions (bifurcation point PB1) while subcritical bifurcation (PB2) leads to unstable bifurcating solutions. Bifurcation points SB1, TB1 and TB2 constitute the junction points for 4 half rays of unstable solutions as shown in diagram e in Figure 11. A point of interest here appears to be the bifurcation point SB2, which looks like a point of higher order singularity in the sense that 3 solution branches seem to exist at this junction probably through multiple (identical) eigen values crossing into right half plane.

3.2. Pattern Formation During Growth

As mentioned earlier, it is important to know the effect of variation in the length of the system, the bifurcation parameter, on the solution evolution process since many biological processes of development, resulting in pattern formation take place in a transient mode. Marek and Kubicek [18] have performed such an analysis for the case of a growing system for the Meinhardt model. By considering a linear and an exponential growth of the domain they have shown how complicated patterns can arise as the length of the system increases with time.

They also suggest that the selection of branches at the bifurcation points is a random process. Their numerical simulations of the transient process, as reported in [18], indicated a rather smooth transition from one solution branch to another while our simulations on the Brusselator model show, in addition, some different behavior. In our studies, we have considered the Brusselator model represented by equations (1) to (3) and used the following linear model to describe the growth process of the system.

$$Z = Z_0 (1 + \alpha t) . \tag{5}$$

Here Z and Z_0 represent the length at a particular time and the original length respectively while t denotes the time and α is the growth constant. If the space domain is nondimensionalized with respect to Z_0 for the purpose of transient simulation, then the effect of increased length is reflected in the value of the diffusion coefficient which changes with time as $D/(1 + \alpha t)^2$. The transient simulation program as mentioned earlier, has therefore been used with an effective (time dependent) diffusion coefficient to analyze the effect of growing system. Since the stability exchange takes place at the bifurcation and the limit points, we have used various bifurcating branches for the purpose of transient simulation (with the starting point close to the bifurcation or limit point).

In a typical transient simulation α was chosen as 0.005, Z_0 as 0.2 and the initial profile had a wave number of 1 (symmetric solution with a negative derivative at the boundary for component Y). According to bifurcation diagrams (1) and (6), the system has 3 stable s. s. at this point (2 are asymmetric solutions corresponding to the branch c and a symmetric profile from branch a). Of these possible choices, the system settled on branch a. Apparently a symmetric perturbation/state leads to symmetry. This branch was followed till $Z = 0.3$ where a stability exchange occurred at the bifurcation point E_1. The continuing branch is unstable so also is the eminating solution. Beyond this point, the system, however, settled again on the previous branch. The path of the solution for this case is shown in Fig. 13 (a) where the almost vertical line shows the behavior near the limit point. In order to compare the effect of growth rate, the solution path, corresponding to $\alpha = 0.0025$ has also been shown in the same figure. It is apparent from this figure that different Z values are required to stabilize the solution on the same branch and this fact can play an important role in the development processes. For example, if the system had one more bifurcation point in between these 2 lengths, the fate of the system could have been totally different. In order to study the system behavior near the bifurcation point E_1 let us superimpose Figs. 1 and 6. It is seen that around E_1, there are 3 stable s. s.

Two correspond to the asymmetric branch c and one results from the branch a (on which the system finally continues). It is logical to expect that the unstable solution will be attracted to the nearest stable branch. Further, an increase in length at the bifurcation point tantamounts to applying a perturbation, which, in this case, happens to be symmetric and the symmetric unstable solution tries to grow in a symmetric fashion. If the relaxation time (i.e. time required by the system to attain steady state) is low, then the evolution process is described by the linear theory and the result can be a symmetric solution. This is what apparently takes place for the case considered. So far, we have analyzed the effect of growing system in a deterministic fashion. However, in real situations, the system may be subjected to random perturbations and in order to simulate this behavior, we have applied concentration perturbations, generated via a random number generator, to the 'system' near the bifurcation point and studied the resulting behavior. The magnitude of the perturbations was chosen to be about 0.1% of the concentration values. A typical result of the simulation is shown in Fig. 13a where the line with small circles indicates the behavior of the perturbed system. No dramatic effect due to fluctuations could be observed. However, as mentioned earlier, the effect of fluctuations may become significant if two solution branches are close to one another and are 'similar'. Such a situation arises near the bifurcation points when the bifurcating solution branch is stable on either side and a finite perturbation can decide the fate of the emanating solution. We have further simulated the behavior of system in growth also with continuously applied perturbations. However, the result in each case, though quantitatively different was qualitatively similar. In a different case, a smooth transition to the original branch a near the bifurcation point J_1 has been depicted in Figure 13b. This smooth transition to the alternating branch also indicates

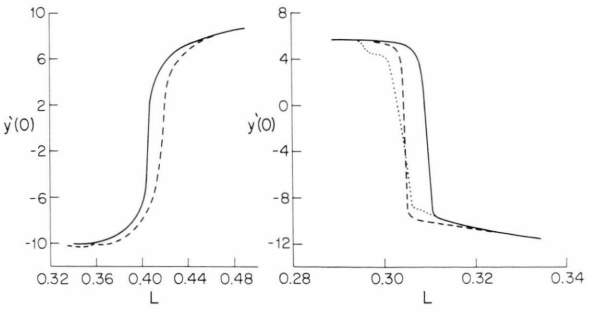

(a) (b)

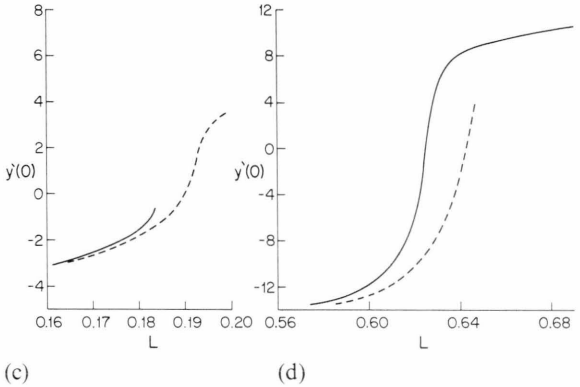

(c) (d)

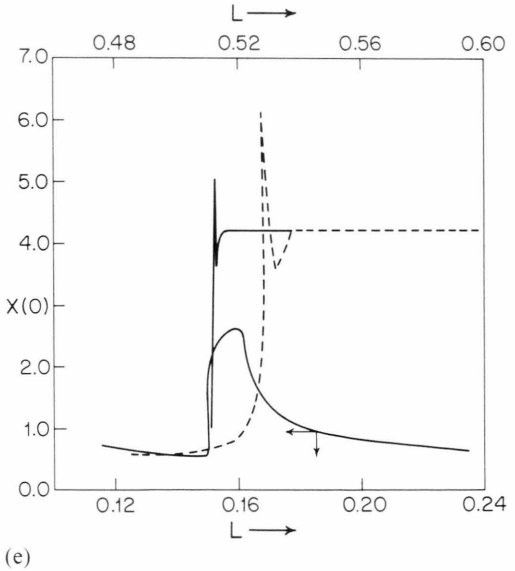

(e)

Fig. 13. Solution behavior for growing system near bifurcation points. —— $\alpha = 0.005$, --- $\alpha = 0.0025$. For Fig. 13(e) —— $\alpha = 0.0025$, --- $\alpha = 0.005$.

that the eigenvalues at the bifurcation point are real. The effect of growth rate, as per expectations is qualitatively similar. The results of analysis near the bifurcation point C_1 are shown in Figure 13c. In this case, the simulation was started on the stable portion of branch b with Z_0 around 0.16 (Fig. 6). For $\alpha = 0.001$, the unstable symmetric solution on branch b switched to the asymmetric branch c. However, for $\alpha = 0.0025$, initially a transition occurred to the asymmetric profile which later changed to the symmetric branch a (Fig. 7). The selection of upper or lower branch at the bifurcation point C_1 is decided by fluctuations and different branches were obtained by applying perturbations near the bifurcation point. The transient simulations on branch c yielded branch g (Fig. 5) when started on either side (negative or positive derivative for $Y'(0)$) of the bifurcation point C_1. The smooth transition from the lower branch of curve c to the upper branch g has been depicted in Figure 13d. For the case of relatively high growth rates, $\alpha = 0.05$, the transient simulation yielded branch g from the curve c but the solution did not conform to branch g till a length of 0.8 was reached. For this case, the time scales of the growth process and the reaction-diffusion system are apparently similar.

The analysis, for the case of zero flux boundary conditions, showed oscillatory behavior at the limit point (near bifurcation point SB2) on branch b (Figure 12). The path of the solution, near this limit point, has been shown in Fig. 13e for $\alpha = 0.0025$ as well as $\alpha = 0.005$. From a mathematical point of view, a complex eigenvalue produces this result. However, in physical situations, its consequences could be important. For example, in a chemical engineering context, the variable X could be the temperature and it may attain values which are much more than those reported in the s. s. bifurcation diagram or which may even be more than the adiabatic temperature rise. As expected, a low growth rate, though it also shows oscillatory behavior quickly settles the system on the stable branch a. Other conclusions, observed for this case are quite similar to those noted for the fixed boundary conditions. For example, a random perturbation at the primary bifurcation point PB1 (Fig. 12) can decide the selection of upper or lower branch c, or affect the smooth transition, observed in switching from the branch b to branch c, as depicted in Figure 13e.

In conclusion, it therefore appears that a stability analysis of the bifurcation diagram alone cannot decide the state of the system in growth. Further, the representation of the state of the system by a derivative at the boundary or a fixed point in space, though qualitatively correct does not quantify the average properties, and nearness of solutions on such a bifurcation diagram (for the distributed parameter system) needs to be properly defined. The important role of growth rate in deciding the destination of the system and the transient effects observed during the evolution process can have important biological implications.

3.3. Effect of Localized Heterogenities on System Behavior

As mentioned earlier in the introduction, inhomogenities have been shown to lead to many interesting effects. Amongst these are asymmetric steady states over catalyst surface, aperiodic and chaotic oscillations in catalytic reactions and oxidation-reduction waves in the Belousov-Zhabotinsky reagent. Sheintuch and Pismen [19] have shown that surface inhomogenities over a catalyst surface can give rise to local oscillators, a combination of which may result either in a train of trigger waves or into a stationary inhomogeneous state, depending upon the mechanism of communication. The effects of heterogenities are also important in a biological context since its presence may affect the development of dissipative structures (order and rhythm).

In the present study with the Brusselator model, we consider heterogenity to be a location in the system, where the kinetic constants may be significantly different than those in the rest of the system. Such a situation can arise, for example, in the context of a biological deactivation. Though it is not very clear as to how such a deactivation occurs, the loss of activity of certain enzymatic systems in catalyzing chemical reactions has been experimentally observed. In our analysis we make a further simplifying assumption that the heterogenity modifies all kinetic constants for the Brusselator model equally. As a result, the nonlinear source term in the reaction-diffusion equations (1) to (3) is modified by a constant factor. This factor can take values from 0 (for a poisoned spot) to very large values (more active locations).

Since the analysis of a distributed parameter system (partial differential equations) is complicated, we initially study the effect of heterogenity for a relatively simple case of two coupled cells (lumped parameter system). A detailed study of such a configuration for the periodic solutions has been performed by Schreiber et al. [20] and Schreiber and Marek [21], although in a somewhat different context. These authors have observed aperiodic oscillations and small windows of chaos when the controlling parameter was the mass exchange coefficient between the cells. In our investigations we have observed a similar behavior however by varying the kinetic rate constants (heterogenity) in the cells. For the case of two coupled cells, the following equations describe the dynamics of the Brusselator model:

$$\mathrm{d}X_1/\mathrm{d}t = A_1 + X_1^2\, Y_1 - (B_1 + 1)\, X_1 + K_x\, (X_1 - X_2)\,, \tag{6}$$

$$\mathrm{d}\, Y_1/\mathrm{d}t = B_1\, X_1 - X_1^2\, Y_1 + K_y\, (Y_1 - Y_2)\,, \tag{7}$$

$$\mathrm{d}X_2\mathrm{d}t = \xi\, (A_2 + X_2^2\, Y_2 - (B_2 + 1)\, X_2) + K_x\, (X_2 - X_1)\,, \tag{8}$$

$$\mathrm{d}\, Y_2/\mathrm{d}t = \xi\, (B_2\, X_2 - X_2^2\, Y_2) + K_y\, (Y_2 - Y_1)\,. \tag{9}$$

While deriving these equations it has been assumed that components A and B are maintained constant in each tank by some external means and a permeable device between the cells allows components X and Y only to diffuse. In order to reduce the number of variables, the exchange coefficients K_x and K_y have been treated as equal in the numerical calculations. The parameter ξ in equations (8) and (9) represents the effect of heterogenity. For the above mentioned configuration, we intend to study the effect of ξ and coupling on the dynamics for the following cases (as decided by the values of the chosen parameters A_1, A_2, B_1, and B_2).

(1) Cell 1 in steady state (s. s.) mode while the cell 2 is in a periodic state and
(2) both cells are in periodic states.

The system of nonlinear ordinary differential equations, represented by (6) to (9) has been solved by the GEAR stiff integrator. In general, the code did not work well for high values of the exchange coefficients. For case (1) the following parameter values have been chosen $A_1 = A_2 = 2.0$, $B_1 = 4.6$, $B_2 = 5.8$, $K_x = K_y = 0.1$ and $\xi = 1.0$.

A linear stability analysis easily shows the cell 1 to be in a s.s.mode while the cell 2 oscillates. Figure 14 a

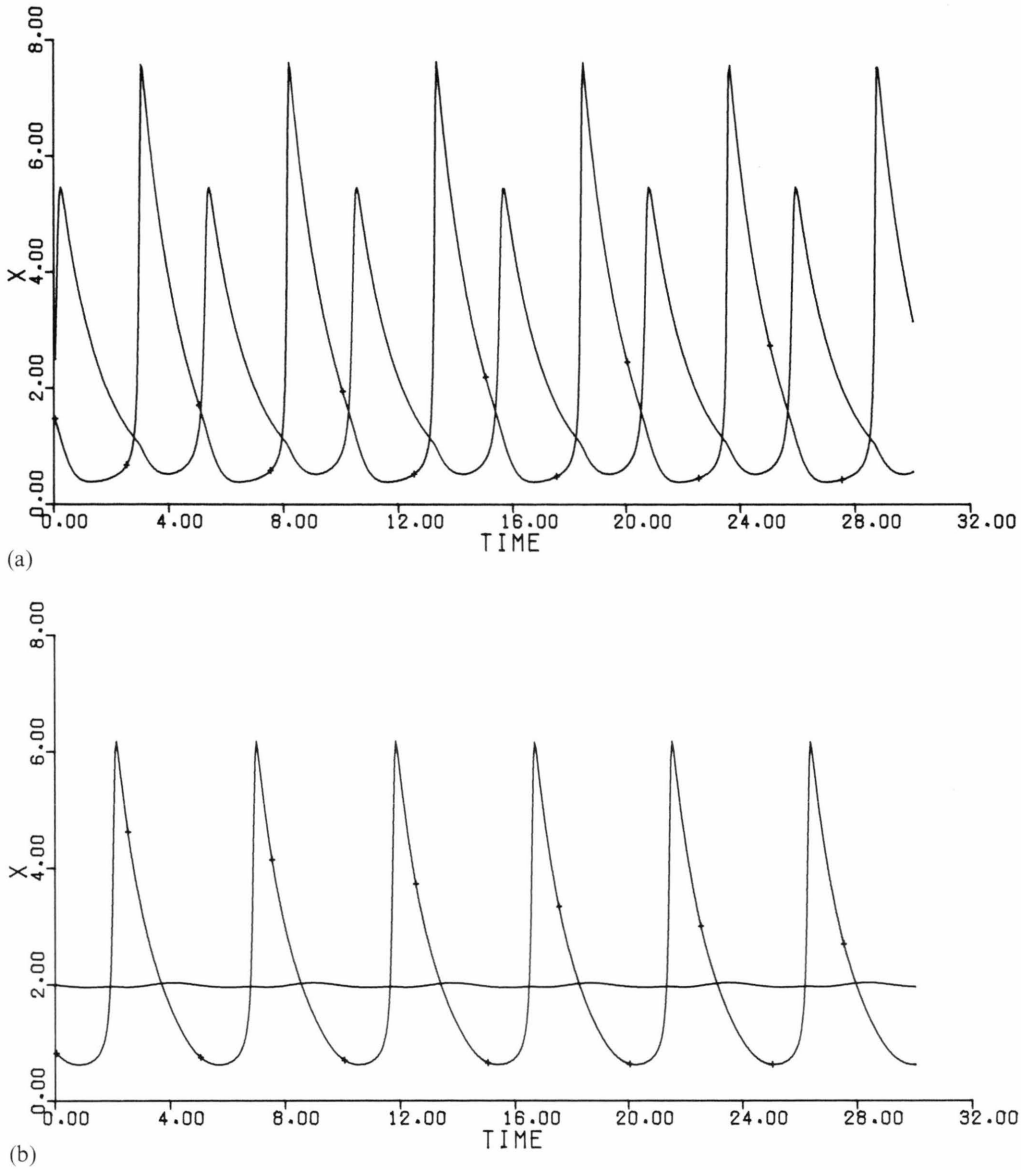

Fig. 14. Oscillations for component X in coupled cells. (a) $K = 0.1$, (b) $K = 0.01$; —— component X_1, —+—+— component X_2.

shows the oscillations induced in cell 1 due to the periodicity in cell 2. The result is not surprising. Since components A and B are maintained constant in individual cells, each cell acts independent of another and the oscillations in the cell 2 get superimposed on cell 1. The combination of a s. s. and a periodic mode therefore results in a periodic motion for the combined system. As a result of synchronization, each cell has the same period of oscillation. In another situation, when $K = 0.01$ (other parameters maintained constant), the combined system again shows oscillations (Fig. 14 b). However, the amplitude of oscillations for the cell 1 is extremely small (a weak interaction between the cells) and the oscillations are bimodal showing an apparent bifurcation of the limit cycle.

In these calculations ξ has been chosen as unity and the observed results are similar to those reported by Schreiber et al. [21]. However, when ξ was increased to 10, disorderly and irregular oscilla-

tions were observed for the component X in cell 2 which have been shown in Figure 15c. On the contrary, the oscillations for the component X in cell 1 were fairly regular. A systematic effect of increasing ξ on the oscillations in cell 2 is shown in Fig. 15, and one may note the loss of stability of a single period limit cycle to limit cycles of increasing complexities (higher periods). We have not performed the detailed stability analysis of these periodic solutions via the Floquet theory, but it is conjectured that one of the multipliers in addition to the first being 1 crosses unit circle when ξ exceeds a critical value. The observed results for the case (2), when either cell operates in a periodic mode, are qualitatively similar to the case (1) i.e. regular oscillations for the component X in cell 1 while increasingly complex oscillations for the component X in cell 2 with increasing ξ. These results are reported in Fig. 16 where one can note the out of phase concentration waves for components, X_1 and X_2 when starting from different initial conditions. The multiple period oscillations, observed in this study, can be explained on the basis of two time scales in the system. For this pupose, we rewrite equations (6) and (8) in the following form:

$$dX_1/d\tau = \varepsilon\,(A_1 + X_1^2\,Y_1 - (B_1+1)\,X_1) + \varepsilon\,K_x\,(X_1 - X_2)\,, \tag{10}$$

$$dX_2/d\tau = (A_2 + X_2^2\,Y_2 - (B_2+1)\,X_2) + \varepsilon\,K_x\,(X_2 - X_1)\,, \tag{11}$$

where $\varepsilon = (\xi)^{-1}$ and $\tau = t\,\xi$ is the stretched coordinate. From equation (10) one can note that component X_1 changes very slowly as compared to the component X_2 and if K_x is of the order of ε, over small τ values we can rewrite (10) as

$$dX_1/d\tau \cong 0. \tag{12}$$

In a similar fashion we can write that $d\,Y_1/d\tau \cong 0$.

This is analogous to the quasi steady state approximation and one can integrate equations for X_2 and Y_2 with X_1 and Y_1 decided from the corresponding algebraic equations. Alternately, one can also view this situation as a single cell with periodic inputs for components X and Y. The equations (11) and (9) then have periodic inputs (nonautonomous systems). For such a situation Tomita and Kai [22] have reported a chaotic behavior of the dependent variables. They have considered the case of a 'forced' Brusselator model in a cell, in which, the differential equation for the component X has a periodic input of the type $a\cos\omega t$ while component Y has no external modulation. In our case, the situation of periodic inputs arises naturally and both components have external excitations. We have, therefore, numerically experimented with the following pair of equations.

$$dX/dt = A + X^2\,Y - (B+1)\,X + C_1 \sin\omega t\,, \tag{13}$$

$$dY/dt = B\,X - X^2\,Y + C_2 \sin\omega t\,. \tag{14}$$

For the few chosen values of C_1, C_2 and ω, we have calculated different types of attractors and a typical (strange) attractor has been reported in Figure 17. A systematic analysis of the problem was out of scope since there are too many parameters in the model. However, it was noted that initial conditions are very sensitive in determining the type of attractors.

In the analysis mentioned so far, K_x and K_y have been treated as constants, independent of composition. However, in a more realistic situation, they may depend upon composition, which can affect the bifurcation behavior of the system. The exchange coefficients here are analogous to the diffusion coefficients, which have been known to depend on composition. Sheng and Nicolis [23] and Nandapurkar and Hlavacek [24] have reported that a concentration dependent diffusion coefficient affects the onset of bifurcation both for s. s. as well as periodic solutions and the stability properties. Similar to the diffusion coefficients we choose the following composition dependence for K_x and K_y

$$K_x = \bar{K}_x\,(1 + \delta X) \quad \text{and} \quad K_y = \bar{K}_y\,(1 + \delta Y)\,.$$

We select $A_1 = A_2 = A$ and $B_1 = B_2 = B$ in such a way that either cell operates in a steady state mode, and study the effect of δ on the Hopf bifurcation parameter B. For the computation of the Hopf bifurcation points, a code developed at SUNY at Buffalo [25] has been used. For $A = 2.0$, the Hopf bifurcation sets in at $B = 5.0$ for the individual cells. For the combined system, Figs. 18a and b show the calculated values of the Hopf bifurcation parameter B as a function of δ at constant values of $\bar{K}$ and ξ. One can easily observe that a stronger dependence of K on δ tends to induce oscillations at a lower value of B while higher values of ξ tend to dampen the effect of δ on the Hopf bifurcation parameter. Further, high values of ξ and low δ brings the combined system behavior to that of a single cell.

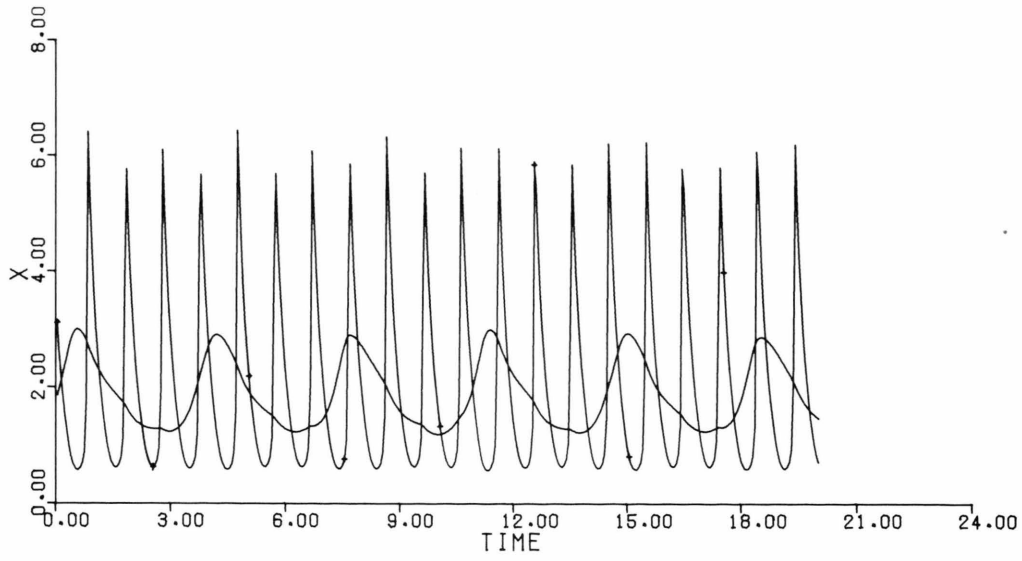

(a)

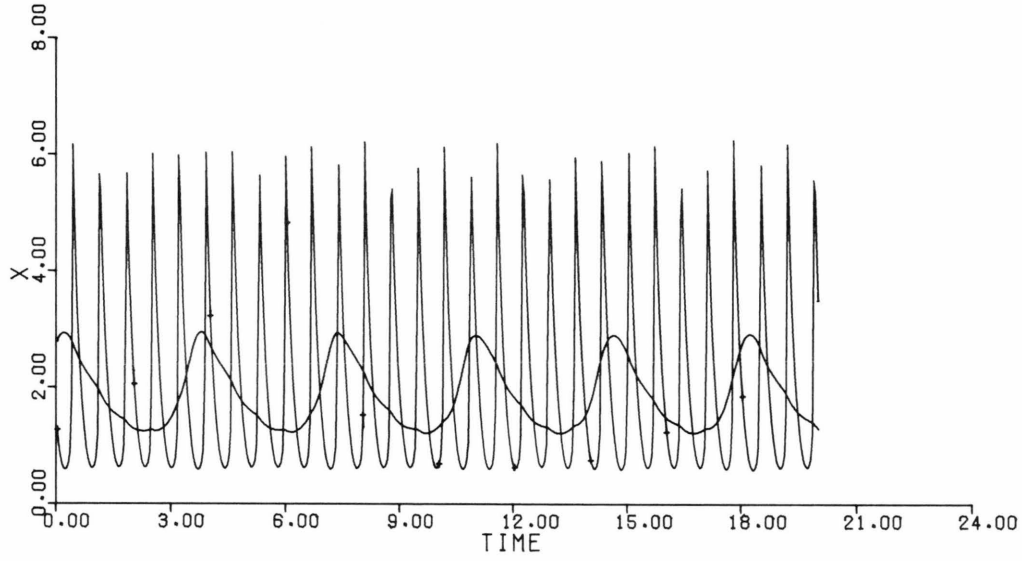

(b)

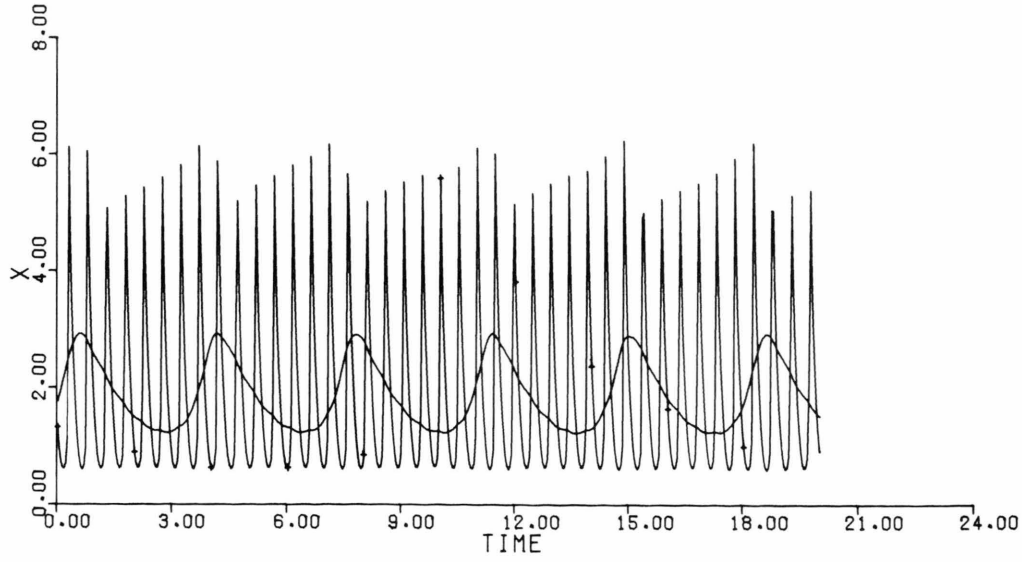

(c)

Fig. 15. Effect of ξ on the nature of oscillations. —— component X_1, — + — + — component X_2. (a) $\xi = 3.0$, (b) $\xi = 7.0$, (c) $\xi = 10.0$, $K = 0.1$ for all calculations.

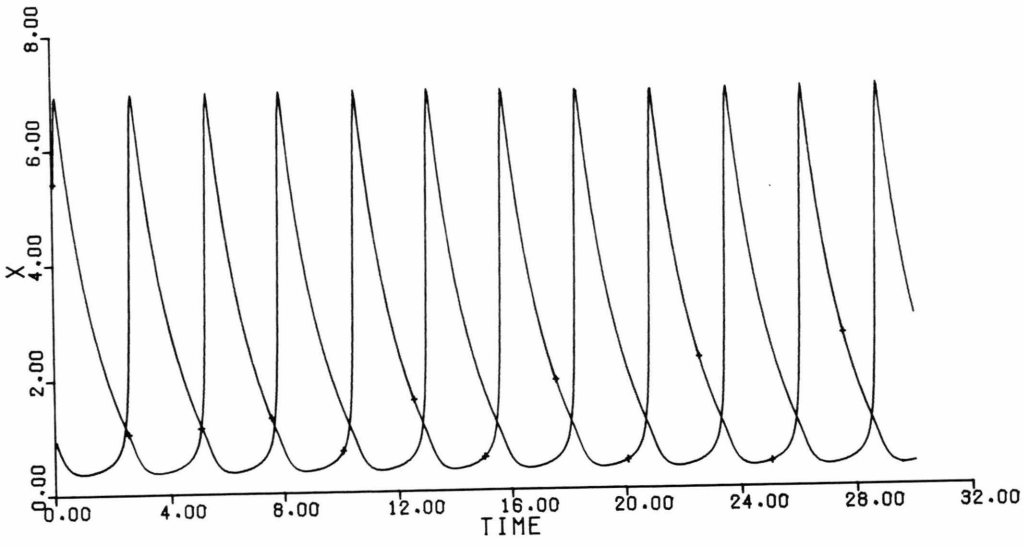

(a)

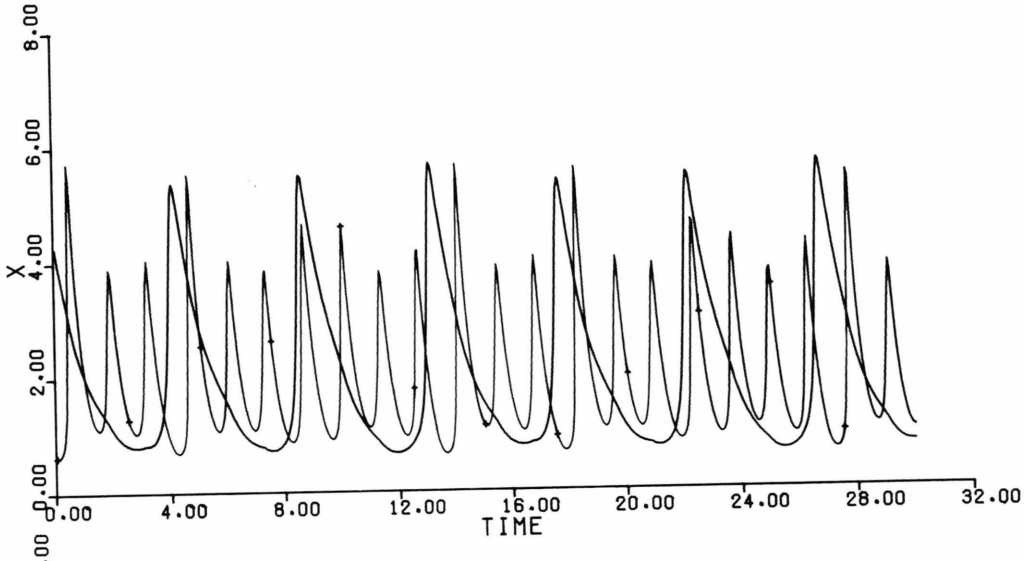

(b)

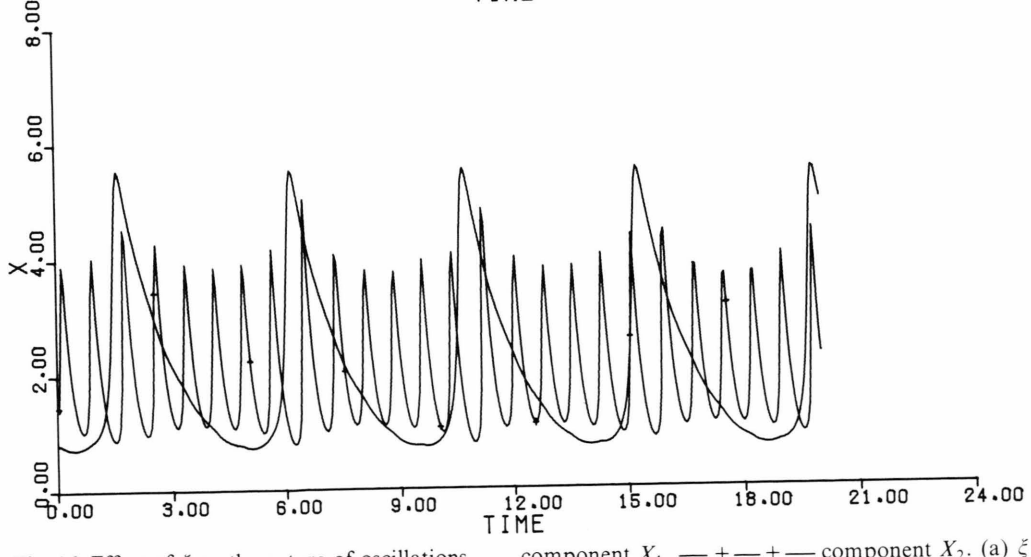

(c)

Fig. 16. Effect of ξ on the nature of oscillations. —— component X_1, — + — + — component X_2. (a) $\xi = 1.0$, (b) $\xi = 5.0$. Parameters: $A_1 = A_2 = 2.0$, $B_1 = B_2 = 5.4$, $K = 0.1$.

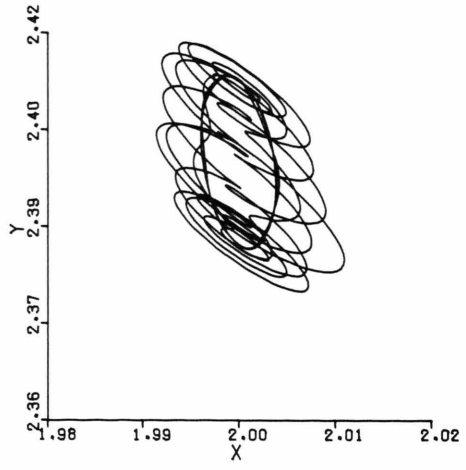

Fig. 17. A strange attractor observed for a cell with a periodic input. Parameters: $C_1 = 0.05$, $C_2 = -0.05$, $\omega = 0.3$.

The reason for this behavior could be the fact that at high ξ values the kinetic term in (8) and (9) can significantly exceed the mass exchange term, i.e.

$$\xi\,(BX - X^2 Y) \gg \bar{K}_y (1+\delta)\,(\Delta X) \quad \text{and}$$
$$\xi\,(A + X^2 Y - (B+1)\,X) \gg \bar{K}_x (1+\delta)\,(\Delta Y)\,.$$

Under these conditions, the differential equations describing the combined system become independent (uncoupled) and the bifurcation behavior, obviously resembles that of a single cell.

With these preliminary results on the behavior of two coupled cells, we now investigate the behavior of a distributed parameter system with heterogenity. In a certain sense, the distributed parameter system is a combination of an infinite number of coupled cells and it would be of interest to see if some similarities in behavior could be noticed between these systems. As can be intuitively expected, the structure of the s. s. solutions, the stability of the periodic solutions and the nature of the periodic solutions is expected to be affected. We use the same transient simulation program, as mentioned earlier in Sect. 3.1 for numerical calculations. The inclusion of heterogenity in the description of the system makes the basic solution of the kinetic equations dependent on space as shown below in (15) and (16).

$$\partial X/\partial t = \xi(z)\,\{A + X^2 Y - (B+1)\,X\} + D_x \nabla^2 X\,, \tag{15}$$

$$\partial Y/\partial t = \xi(z)\,\{BX + X^2 Y\} + D_y \nabla^2 Y\,. \tag{16}$$

$\xi(z)$ may be a discontinuous function of the space coordinate in (15) and (16). The bifurcation analysis, as reported in [6, 7] cannot, therefore, be applied here. In this case, one has to resort to the numerical analysis of the problem. Our idea here is to show the effect of a localized heterogenity on the formation and development of patterns and we consider few cases to show this effect rather than construct the complete bifurcation diagram. Figure 19 shows a typical result obtained via the transient simulation. Here we consider a single heterogenity at the centre of the system and ξ has values of 1 (isotropic case), 0 and 10. We start from the same initial profile in all the 3 cases and the s. s. solution obtained at $t \to \infty$ have different characteristics showing thereby that a single heterogenity can excite different eigenmodes and affect the long-term behavior. As obviously expected, for $\xi = 0$ the gradients at the centre are zero. However, for the same set of parameters and the initial profiles when diffusion of component A is taken into considera-

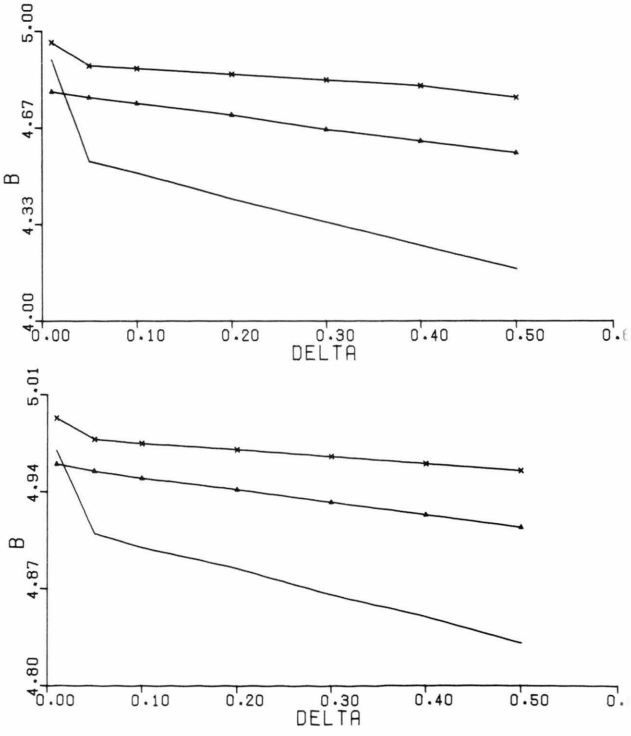

Fig. 18. Effect of nonlinear mass exchange coefficient on Hopf bifurcation. Parameters: $A_1 = A_2 = 2.0$; —×— $\xi = 0.25$; —▲—▲— $\xi = 1.0$; — $\xi = 3.0$.
(a) $\bar{K} = 0.05$; (b) $\bar{K} = 0.01$.

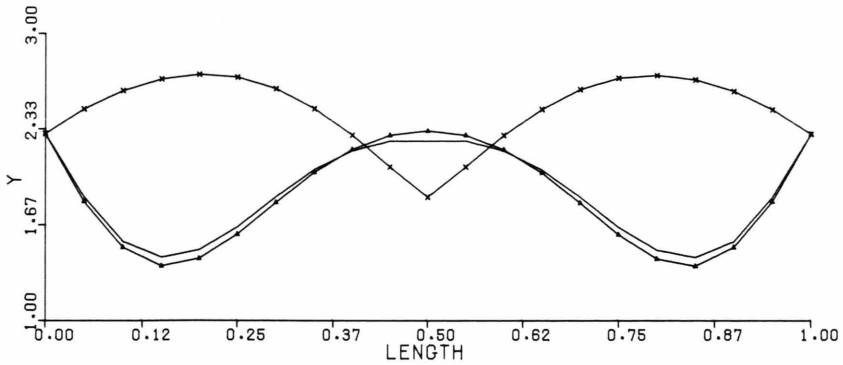

Fig. 19. Effect of spatial inhomogenity on steady state solutions. $A = 2.0$, $B = 4.6$, $D_x = 0.0016$, $D_y = 0.008$, $L = 0.3$; —— $\xi = 0$; —▲—▲— $\xi = 1.0$; —×—×— $\xi = 10.0$.

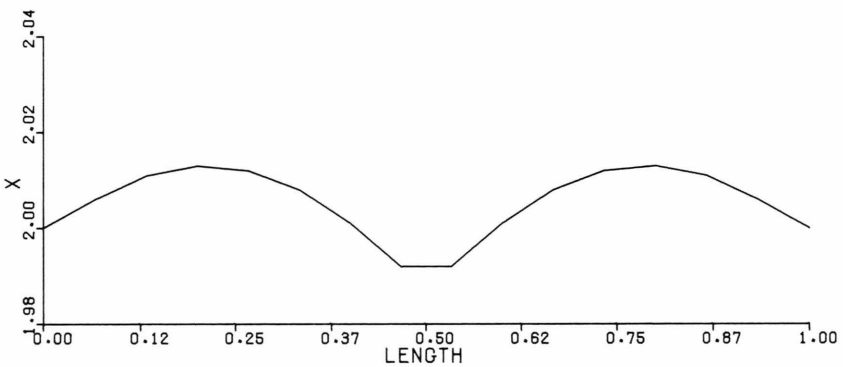

Fig. 20. Stability change of a periodic solution to a s.s. solution. $A = 2.0$, $B = 5.4$, $D_x = 0.008$, $D_y = 0.004$, $D_A \to \infty$, $L = 0.6$, $\xi = 10.0$.

tion, no significant qualitative or quantitative effect of heterogenity have been observed (in all cases, the final s. s. solutions are almost the same). In another situation, a single heterogenity at the centre is shown to affect the stability properties of the periodic solutions. For the parameter values $A = 2.0$, $B = 5.4$, $D_x = 0.008$, $D = 0.004$ and $D_A \to \infty$ and for the fixed boundary conditions, the first bifurcation to the periodic solution takes place at $L \cong 0.544$. In our numerical simulations, we have, therefore, used the same set of parameters except $L = 0.6$ and a heterogenity at the center as well as at two other locations. The simulated results are shown in Fig. 20 which depicts a s. s. solution (which is very close to the thermodynamic solution when no heterogenity is present). The same set of parameters, for the zero flux boundary conditions, yield a discontinuous standing wave and the interesting aspects of this periodic solution are its initial transients. The development of this periodic solution from the initial profile is shown in Fig. 21 and one can observe the development of sharp local concentration gradients at the point of heterogenity, which, in some sense look like target center and can have important biological implications. When the diffusion of component A was also considered along with the heterogenity, some interesting numerical observations have been made. In the absence of heterogenity, the diffusion of component A causes concentration fronts to form, propagate from the boundaries towards the center, collide and ultimately change to a standing wave pattern [14]. The presence of heterogenity however causes the development of a sharp concentration gradient at the point of heterogenity (as shown in Figure 22). This front then tries to move in the direction of low concentrations i.e. towards the boundaries. Simultaneously, the kinetics of the overall system tends to take the system near the boundary towards high concentration values, which creates a valley between the center (the point of heterogenity) and the boundary. Thus additional concentration fronts are created as a result of the heterogenity. This type of periodic solution is depicted in Fig. 22 where curves 1–2–3

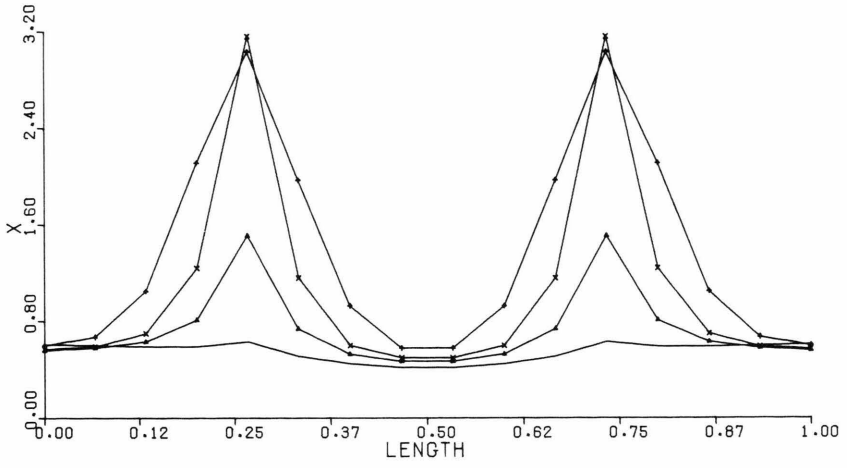

Fig. 21. Initial transients for a periodic solution with spatial inhomogenity. $A = 2.0$, $B = 5.4$, $L = 0.6$, $D_x = 0.008$, $D_y = 0.004$, $\xi = 10.0$, $D_A \to \infty$.

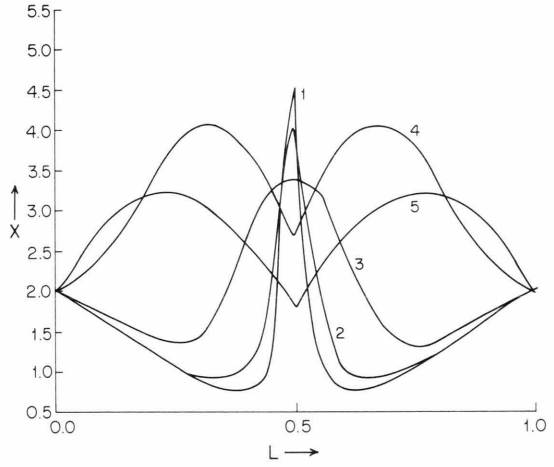

Fig. 22. Periodic solution with diffusion of component A and spatial inhomogenity at center. Fixed boundary conditions. Parameter values are $A = 2.0$, $B = 5.4$, $L = 0.6$, $D_x = 0.008$, $D_y = 0.004$, $D_A = 0.1$, $\xi = 10.0$.

correspond to the concentration front at the center while curves 4 and 5 show the state of the system after the propagation of these concentration fronts.

The effect of heterogenity and zero flux boundary conditions has been found to divide the system into two parts, each part representing a standing wave. The qualitative results of numerical simulation for this case are shown in Fig. 23 which shows that the central portion (heterogenity at the centre, $\xi = 10$) is almost stationary. To explain this behavior, we again make use of multiple time scales in the system. The explanation further needs that concentration gradients in the system, in the absence of heterogenity be low. Such a behavior is observed for standing waves at low system size. Under this situation we neglect the second spatial derivative and obtain the following system of differential equations:

$$\frac{dX_i}{dt} = A + X_i^2 Y_i - (B+1) X_i \quad i = 1, n-1 \quad (17)$$

and

$$\frac{dX_n}{dt} = (A + X_n^2 Y_n - (B+1) X_n) \xi . \quad (18)$$

Here n denotes the point of heterogenity. One can now see that X_n changes over a much shorter time scale as compared to the remaining X_i and can, therefore, be considered as quasistationary. This

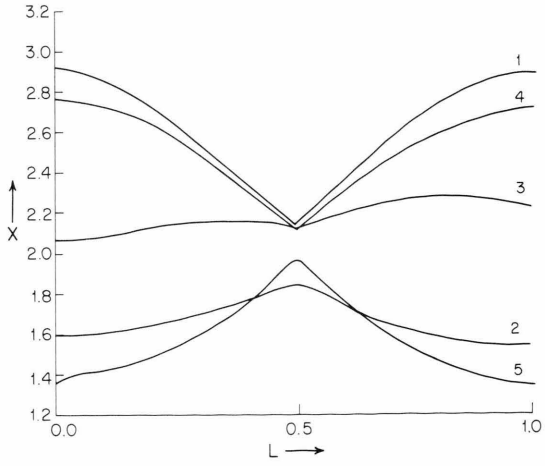

Fig. 23. Partitioning standing waves for zero flux boundary conditions. $A = 2.0$, $B = 5.4$, $L = 0.6$, $D_x = 0.008$, $D_y = 0.004$, $D_A \to \infty$. $\xi = 10.0$ at center.

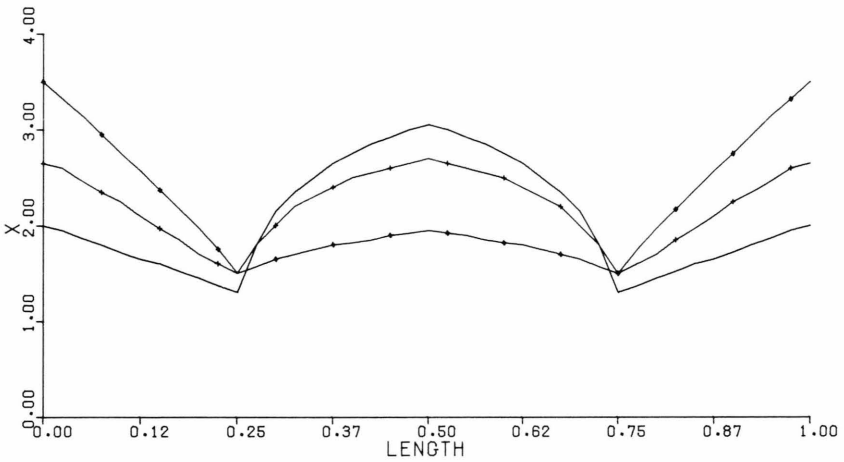

Fig. 24. Effect of 2 heterogeneous locations in the system. Parameter values are as those for Figure 23.

gives rise to the type of periodic solution as shown in Figure 23. By making use of these arguments, we can see that if there are two such heterogeneous locations in the system, the type of periodic solution, for the case of zero flux boundary conditions, would be 3 standing waves. One exists between the 2 heterogeneity locations and one each between the boundary and the heterogenity. The qualitative sketch of this type of solution, which we have numerically simulated, is shown in Figure 24. The explanation offered above does not hold for the case when the composition of component A is dependent on space as it gives rise to concentration fronts, where the spatial derivative could be infinite. Let us extrapolate these arguments further and consider a two dimensional system with such sites of local heterogenities. We will, in this situation, probably observe a configuration consisting of a number of cells, each consisting of a dissipative structure and most likely acting independent of the neighbor.

Conclusions

A combined study of the stability analysis of the bifurcation diagram and the transient simulation of the system in growth reveals the importance of growth rate in the pattern selection process. It also shows the importance of limit and bifurcation points in determining the stability properties. The results suggest that the selection of branches at the bifurcation points may be determined by random perturbations and a stochastic description may be more appropriate here. It is also noticed that the transient effects during the switching of solution branches at the turning points can have important implications. Apriori prediction of pattern selection, on the basis of the stability analysis of the bifurcation diagram, is difficult to make. However, for finite growth rates, it is likely that symmetric solution branches, after the loss of stability, will switch to symmetric solutions, if they are stable. Numerical calculations on coupled cells indicate that a heterogenity in the system can introduce multiple time scales. This apparently causes aperiodic or irregular oscillations. The occurrence of two time scales results in some strange attractors to form in such a system. For a distributed parameter system, the heterogenity can cause development of sharp local concentration gradients, alter the stability properties and can cause partitioning of the system.

[1] A. M. Turing, Phil. Trans. Roy. Soc. London, Ser. B, **B237,** 37 (1952).
[2] I. Prigogine and R. Lefever, J. Chem. Phys. **48,** 1695 (1968).
[3] A. Gierer and H. Meinhardt, Kybernetik **12,** 30 (1972).
[4] E. E. Selkov, Eur. J. Biochem. **4,** 79 (1968).
[5] G. Catalano, J. C. Eilbeck, A. Monroy, and E. Parisi, Physica **3D,** 439 (1981).
[6] J. F. G. Auchmuty and G. Nicolis, Bull. Math. Biol. **37,** 323 (1975).
[7] M. Herschkowitz-Kaufman, Bull. Math. Biol. **37,** 589 (1975).

[8] J. A. Boa and D. S. Cohen, SIAM J. Appl. Math. **30,** 123 (1976).
[9] M. Kubicek, V. Ryzler, and M. Marek, Scientific Papers of the Prague Institute of Chemical Technology, **K14,** 147 (1979).
[10] V. Hlavacek, R. Janssen, and P. Van Rompay, Z. Naturforsch. **37a,** 39 (1982).
[11] R. Janssen, V. Hlavacek, and P. Van Rompay, Z. Naturforsch. **38a,** 487 (1983).
[12] D. A. Sattinger, Topics in Stability and Bifurcation Theory, Springer-Verlag, Lecture Notes No. 309 (1973).
[13] M. Kubicek, M. Marek, P. Hustak, and V. Ryzler, Proceedings of the 5th Symposium: Computers in Chemical Engineering 903 (1977).
[14] P. Nandapurkar and V. Hlavacek, Z. Naturforsch. **38a,** 963 (1983).
[15] A. T. Winfree, Science **175,** 634 (1972).
[16] J. J. Tyson and P. C. Fife, J. Chem. Phys. **73** (5), 2224 (1980).
[17] K. F. Jensen and W. H. Ray, Chem. Eng. Sci. **35,** 2439 (1980).
[18] M. Marek and M. Kubicek, Z. Naturforsch. **35a,** 556 (1980).
[19] M. Sheintuch and L. M. Pismen, Chem. Eng. Sci. **36,** 489 (1981).
[20] I. Schreiber, M. Kubicek, and M. Marek, New Approaches to Nonlinear Problems in Dynamics, Ed. P. J. Holmes, SIAM Philadelphia 1980, p. 496–508.
[21] I. Schreiber and M. Marek, Physica **5D,** 258 (1982).
[22] K. Tomita and T. Kai, Prog. Theo. Phys. **64,** 280 (1978).
[23] R. Li and G. Nicolis, J. Phys. Chem. **85,** 1907 (1981).
[24] P. Nandapurkar and V. Hlavacek, Bull. Math. Biol., in press.
[25] B. D. Hassard, N. D. Kazarinoff, and Y. H. Wan, Theory and Applications of Hopf Bifurcation, London Mathematical Society Lecture Notes 41, Cambridge University Press 1981.